

Novel chloroquine loaded curcumin based anionic linear globular dendrimer G2: a metabolomics study on *Plasmodium falciparum* in vitro using ¹H NMR spectroscopy

Research Article

Cite this article: Elmi T, Shafiee Ardestani M, Hajjalilani F, Motevalian M, Mohamadi M, Sadeghi S, Zamani Z, Tabatabaie F (2020). Novel chloroquine loaded curcumin based anionic linear globular dendrimer G2: a metabolomics study on *Plasmodium falciparum* in vitro using ¹H NMR spectroscopy. *Parasitology* **147**, 747–759. <https://doi.org/10.1017/S0031182020000372>


Received: 29 October 2019
Revised: 29 January 2020
Accepted: 17 February 2020
First published online: 27 February 2020

Key words:

Dendrimer G2; malaria; metabolomic; nanocomposite; Protozoa

Author for correspondence:

Fatemeh Tabatabaie, Zahra Zamani, E-mail: tabatabaei.f@iums.ac.ir, iran.zamani@pasteur.ac.ir

Taher Elmi¹ , Mehdi Shafiee Ardestani², Fateme Hajjalilani³, Manijeh Motevalian⁴, Maryam Mohamadi⁵, Sedigheh Sadeghi⁵, Zahra Zamani⁵ and Fatemeh Tabatabaie¹

¹Department of Parasitology and Mycology, Faculty of Medicine, Iran University of Medical Sciences, Tehran, Iran;

²Department of Radiopharmacy, Faculty of Pharmacy, Tehran University of Medical Sciences, Tehran, Iran;

³Medical Parasitology Department, School of Medicine-International Campus, Iran University of Medical Sciences, Tehran, Iran; ⁴Department of Pharmacology and Razi Drug Research Center, Iran University of Medical Sciences, Tehran, Iran and ⁵Biochemistry Department, Pasteur Institute of Iran, Pasteur Avenue, Tehran, Islamic Republic of Iran

Abstract

Due to side-effects and inefficiency of the drugs used in malaria treatment, finding alternative medicine with less side-effects has attracted much attention. In this regard, in the present study, nanocomposite synthesized and its effects on the metabolites of *P. falciparum* were investigated. Subsequent to synthesis of nanocomposites, characterization was carried out using nuclear magnetic resonance (NMR), liquid chromatography-mass spectrometry (LC-MS), scanning electron microscopy, dynamic light scattering and Fourier-transform infrared tests. Solubility and drug release were measured and its toxicity on Vero cell was assessed using the MTT assay. The antiparasitic effect of the nanocomposite on the metabolites of *P. falciparum* was investigated by ¹H NMR spectroscopy. Among synthesized nanocomposites, the average size of 239 nm showed suitable solubility in water as well as slow drug release. The MTT assay showed no toxicity for Vero cell lines. Concentrations of 2.5 $\mu\text{g mL}^{-1}$ of nanocomposite eliminated 82.6% of the total parasites. The most effected metabolic cycles were glyoxylate and dicarboxylate metabolism. In this study, ¹H NMR spectroscopy was used with untargeted metabolomics to study the effect of the nanocomposite on *P. falciparum*. Playing an essential role in understanding drug-target interactions and characterization of mechanism of action or resistance exhibited by novel antiprotozoal drugs, can be achieved by targeting metabolic using LC-MS.

Introduction

Malaria is a life-threatening disease that affects human and animals. Four different species of *Plasmodium* cause malaria in human, including *P. falciparum*, *P. vivax*, *P. ovale* and *P. malariae*. Although human patients are sometimes infected with animal pathogens of *Plasmodium*, such as *P. knowlesi* (Antinori *et al.*, 2012; Elmi *et al.*, 2019). The disease caused by *P. falciparum* in human is the most dangerous and fatal as compared with other species. In 2018, there were an estimated 405 000 deaths from malaria globally, compared with 416 000 estimated deaths in 2017 and 585 000 in 2010 (WHO, 2019).

The drugs used to treat malaria, artemisia annua, primaquine, chloroquine, mefloquine and lumefantrine have shown side-effects such as anorexia, stomach ache, diarrhea, nausea, vomiting and visual disturbances. Also, some of these drugs are contraindicated in pregnancy, kids and G6PD deficient subjects. The side-effects of drugs as well as drug resistance observed in parasite, raised some problems in their application, hence raising the need for an alternative medicine (Braga *et al.*, 2015; Guo, 2016; Ghimire *et al.*, 2017). To improve the efficiency of anti-malarial drugs, nowadays, the combination therapy is recommended. Artesunate plus amodiaquine or amodiaquine plus sulfadoxine-pyrimethamine is more commonly used therapies. Although the synergistic effects of drugs cause a better therapy, but their side-effects may also increase. Thus, finding a new nanodrug combination with herbal-chemical nature may reduce the risk of unintended side-effects in patients (Tagbor *et al.*, 2006; Faye *et al.*, 2007; Lu, 2015).

Currently, the nanotechnologists have created carriers to improve drug effectiveness. Studies carried out on antibiotic loaded on nanoparticles have shown their enhanced antibacterial effect and when different drugs including amphotericin B were loaded on nanoparticles, less nephrotoxicity has been reported (Mukherjee *et al.*, 2016; Zia *et al.*, 2017). Recently, there has been a growing interest in the use of dendrimer as a nano-drug carrier (Namazi *et al.*, 2011).

Dendrimers are nanometre-sized, highly branched molecules with highly regulated structure and end groups located on the peripheries. The spaces between its branches are favourable for drug encapsulation (Lo *et al.*, 2013; Abbasi *et al.*, 2014). The biocompatible and biodegradable dendrimer of citric acid–polyethylene glycol–citric acid (CPEGC) is a good candidate of these types, which its 1–3 generations as drug delivery systems were synthesized by Namazi and Adeli (2003) and the controlled delivery of mefenamic acid and diclofenac with these carriers is already examined (Namazi and Adeli, 2005). These dendrimers are biocompatible, have high potential as carriers in drug delivery, and increase drug solubility if combined with hydrophobic drugs (Haririan *et al.*, 2010). However, the represented synthesis method for these dendrimers is difficult and needs various steps for purification which is time consuming and reduces efficiency. Furthermore, the harmful and toxic substances such as dichloromethane and diethyl ether were used in its synthetic pathway (Alavidjeh *et al.*, 2010; Haririan *et al.*, 2010). Therefore, this study is conducted with the aim of finding a new and simple method, without using toxin and harmful materials, for the synthesis of CPEGC of second generation (G2). One of the herbal drugs that has been approved for its anticancer, antibacterial and anti-parasitic effect is curcumin. Curcumin is the active compound in *curcuma longa* which, due to its low hydrophilicity, has faced troubles in pharmacological applications. Various strategies were used to improve the solubility of the drug, namely the use of high-water soluble nanodendrimers (Tyagi *et al.*, 2015; Tiwari *et al.*, 2017; Rahmani *et al.*, 2018).

Conjugation of chloroquine with this nanocomposite was anticipated to increase its effectiveness on the plasmodium parasite. Since nanodendrimer G2 increases drug uptake by cells, they require lower dosages to have the same anti-parasitic effects, hence reducing the side-effects (Tallarida, 2011). On the other hand, if there is a synergistic effect between curcumin and CQ, the new drug combination, at a lower dose, will have a greater effect on plasmodium parasite. In the current study, with the aim of assaying the effects of the synthesized nanocomposite on plasmodium parasite, the parasite metabolic profile was studied by the ^1H NMR method, and then compared with the control group. The most important advantage of studying metabolomics (metabolomics method) over other methods is the simultaneous and network analysis of metabolites and the study of the relationships between metabolites (Tyagi *et al.*, 2015; Tiwari *et al.*, 2017; Mehrizi *et al.*, 2018).

The found results might be useful in achieving specialized markers, for finding new and effective drug targets, in treating fatal disease of malaria. The present study aimed to examine the nanocomposite effect of G2 dendrimer + curcumin + chloroquine (NDC-CQ) on *P. falciparum* *in vitro*. The aim of the present study was to synthesize a novel chloroquine based anionic linear globular dendrimer-curcumin nano-conjugate and investigation of its antiplasmodial effect on metabolome of *P. falciparum* by pFLDH assay and ^1H NMR-based metabolomics analysis.

Materials and methods

Nanocarrier synthesis

First, nanodendrimer G2 (ND) was synthesized using the modified method of Namazi and Adeli (2005) (2 mL of polyethylene glycol 600, 5 mL dimethyl sulfoxide, 1.2 g N, N'-dicyclohexylcarbodiimide and 1.2 g citric acid). In order to conjugate curcumin to nanodendrimer G2 (NDC) as a nanocarrier, 100 mg curcumin was added to 500 mg nanodendrimer G2 in ethanol. A total of 2.2 mg calcium chloride with 280 mg 1-ethyl-3-(3-dimethylaminopropyl)carbodiimide was added to

the compound. The reaction was completed under reflux reaction at 110°C after 72 h. The solutions were removed by a rotary evaporator, and using chromatography G-75 (MERCK, Germany), nanocarrier was purified. Finally, the resulting solution was lyophilized to obtain a dry powder.

Novel nanocomposite synthesis

To synthesize the novel chloroquine-based anionic linear globular dendrimer–curcumin nano-conjugate (NDC-CQ) as the nanocomposite, CQ was loaded into the nanocarrier (Mehrizi *et al.*, 2018). A total of 100 mg synthesized nanocarrier was dissolved in 4 mL ethanol (70%), and then 40 mg CQ was added to solution and rotated for 7 days. The achieved solution was then centrifuged with $21\,728 \times g$ for 30 min. The sediment was then washed with PBS 1× three times and lyophilized. Different dilutions of the finalized novel nanocomposite were prepared to assess their anti-malarial effects.

Using spectroscopic analysis, the absorption ratio of different dilutions of curcumin and CQ was recorded and the respective standard curve was drawn. The loading percentage was then calculated after using a NanoDrop set at a wavelength of 429 nm to assess the absorption of 100 mg mL^{-1} of the nanodrug (Bruni *et al.*, 2017; Mehrizi *et al.*, 2018).

$$\text{Drug loading efficiency \%} = \frac{\text{Initial drug} - \text{drug in supernatant}}{\text{Initial drug}} \times 100$$

Nanocomposite characterization

Determining form, size and distribution of the particle was carried out using dynamic light scattering (DLS) and scanning electron microscope (SEM). The nanodendrimer G2 was confirmed by using liquid chromatography-mass spectrometry (LC-MS). Further, nuclear magnetic resonance (NMR) in D_2O solution and Fourier-transform infrared (FTIR) spectroscopy were also applied to confirm dendrimer–curcumin conjugate (NDC) and nanocomposite (NDC-CQ) synthesis respectively (Mehrizi *et al.*, 2018).

Nanocomposite solubility and cellular absorption

To calculate nanocomposite solubility, 1 mg free curcumin, CQ and synthesized nanocomposite were prepared in water and after centrifugation and removal of the sediments, their absorption were measured in wavelengths of 200–800 by a NanoDrop set. Flow cytometry (FCM) was used to determine the amount of drug uptake by cells. Untreated cells were used as the negative control group.

Drug release

Dialysis sets were utilized in pH 7.4 and various time periods to record the nanocomposite release rate. The amount of the nanocomposite released was assessed using spectrophotometry and utilizing the relative standard curves.

Hemolytic assay

The protocol provided by Memar *et al.* (2016) was employed for hemolytic assay of the drug. A total of 5 mL of freshly drawn blood was centrifuged along with 50 μL of EDTA for 10 min at $804 \times g$. The sediment was dissolved in 4 mL of PBS 1× buffer and again was centrifuged for 10 min at $804 \times g$. The final erythrocyte was then dissolved in 80 mL of PBS 1×.

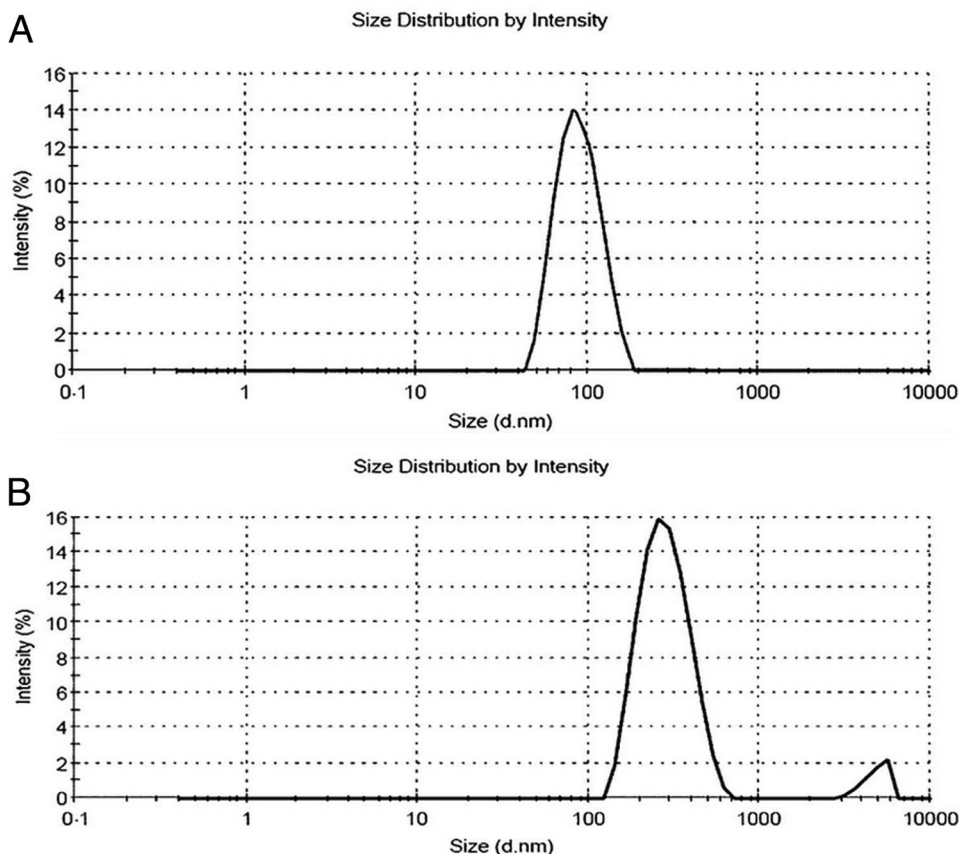


Fig. 1. DLS showing the size distribution of NDC (A) and NDC-CQ (B). Polydispersity index is related to the distribution of the nanocomposite. The polydispersity index (PDI) average was 0.23 ± 0.01 (the PDI value which is close to 0 shows the homogeneous nanoparticle solution while the PDI value above 0.5 indicates the heterogeneous nanoparticle solution).

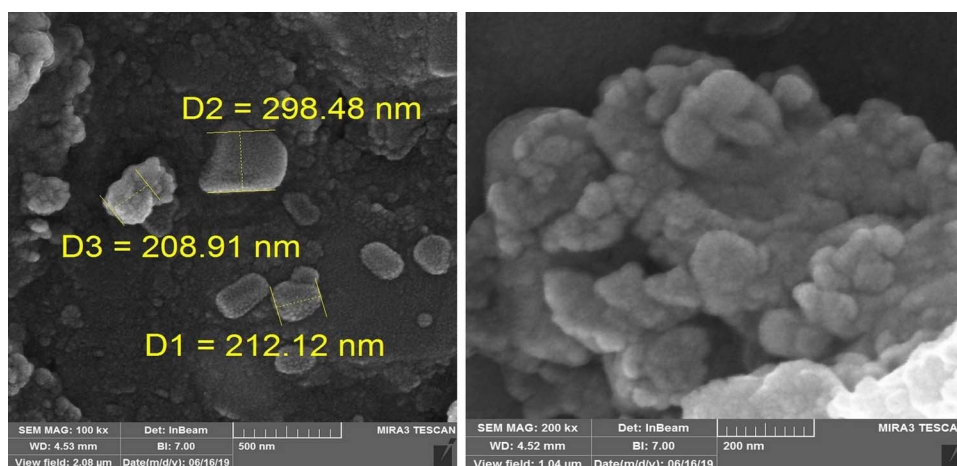


Fig. 2. SEM image of NDC-CQ showed proper morphology with magnification 100 and 200k \times respectively.

A total of 190 μ L blood plus 10 μ L of different dilutions of the nanocomposite were then added to each microplate well. The first well was designated as negative control (PBS 1 \times) and the last one was positive control (triton \times 100). The samples were finally incubated at 37 $^{\circ}$ C for 30 min before measuring their absorption at 540 nm with a spectrophotometer (Memar *et al.*, 2016). The hemolysis percentage was calculated using the following formula:

$$\text{Hemolysis \%} = \frac{(\text{OD test} - \text{OD negative control})}{(\text{OD positive control} - \text{OD negative control})} \times 100$$

MTT assay

Vero cells were provided by Tehran University of Medical Sciences and cultured in DMEM + 10% FBS + 1% PenG/Strep medium. Cell viability was assessed using the MTT assay upon tetrazolium salt decomposition by the mitochondrial succinate dehydrogenase in the live cells. After 48 h of drug introduction to the plates, 10 μ L of MTT solution and 100 μ L of DMSO were added, respectively. Finally, absorbances were read on a microplate reader at 570 nm and at a reference wavelength of 630 nm (Lazaro and Gay, 1998).

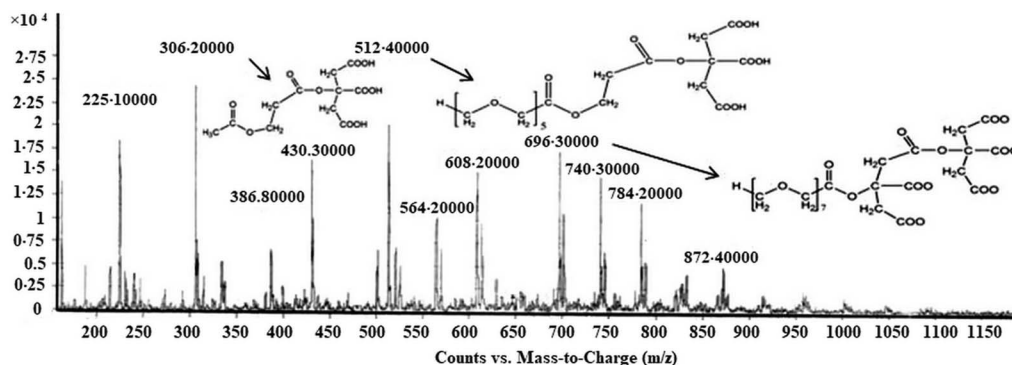


Fig. 3. LC-MS spectrum of dendrimer G2.

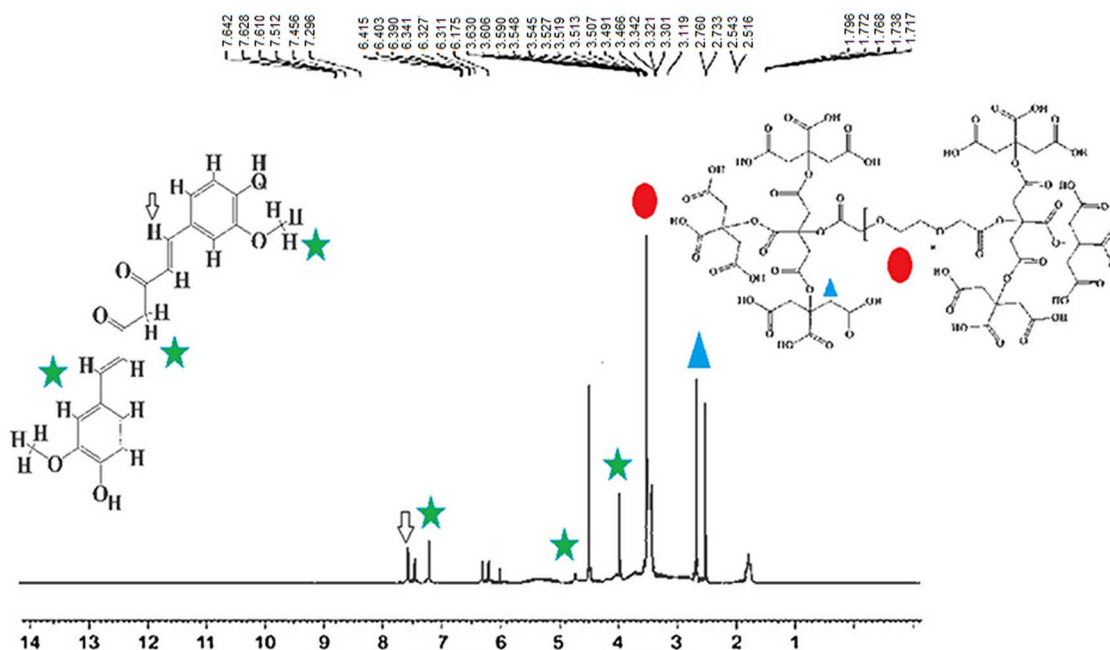


Fig. 4. ^1H NMR spectra to confirm the covalent conjugation of nano-dendrimer to curcumin as the drug carrier (NDC).

P. falciparum culture

The Trager and Jensen (1976) modified method was used to culture *P. falciparum*. Protozoans of *P. falciparum* 3D7 strain were cultured in 7 mL RPMI1640 medium with 10% human serum, hematocrit 2%, HEPES 5.958 g L⁻¹, NaHCO₃ (g L⁻¹), hypoxanthine (13.6 mg L⁻¹), gentamicin (25 g L) and D-glucose (4.5 g L⁻¹). The medium was changed every 48 h, and incubated with CO₂ 5% in 37°C.

Antiplasmodial activity of nanocomposite

After suitable growth of parasite in culture medium (parasitemia 1% and hematocrit 2%) 150 μL of falcon contents were transferred to microplate sinks. Afterwards, 50 μL of various concentrations of drug (0.1, 0.5, 1, 1.5, 2 and 2.5 $\mu\text{g mL}^{-1}$) were added to microplates. The first and final well of the microplate were negative and positive controls respectively. The microplate was finally transferred to a candle jar, and incubated at 37°C for 48 h. The tests were repeated in three microplate rows to confirm the results. Finally, the parasitemia was estimated by the microscopic and enzymatic (pLDH) methods.

Microscopic counting method

Thin smears were prepared from each well and then stained with Geimsa stain to determine the percentage of parasitemia by microscopy.

Lactate dehydrogenase (LDH) assay

Parasitemia was determined by measuring the pLDH activity using spectrophotometry, according to a modified version of the method of Makler and Hinrichs (1993). In summary, 100 μL of Malstat reagent (0.11% v/v Triton-100; 115.7 mM lithium L-lactate; 30.27 mM Tris; 0.62 mM 3-acetylpyridine adenine dinucleotide) with pH 9 and then 25 μL of PES/NBT (1.96 mM nitro blue tetrazolium chloride; 0.24 mM phenazine ethosulphate) were added to each well of a 96-well plate. Finally, 20 μL of a suspension culture medium containing 0.5% parasitemia, 1.5% hematocrit and different concentrations of the nanocomposite were added to the previous solution and the absorbance was then read at 650 nm. The first and last wells were contained the negative (blood without parasites) and positive controls (blood containing parasites), respectively. The percentage of parasitemia was calculated using the following formula:

$$\text{Parasitemia \%} = \frac{(\text{OD test} - \text{OD negative control})}{(\text{OD positive control} - \text{OD negative control})} \times 100$$

Isolation of parasites

To purify the ring stage of *P. falciparum* (isolation of parasites), the test flask contents were centrifuged at 289 $\times g$ for 5 min, the

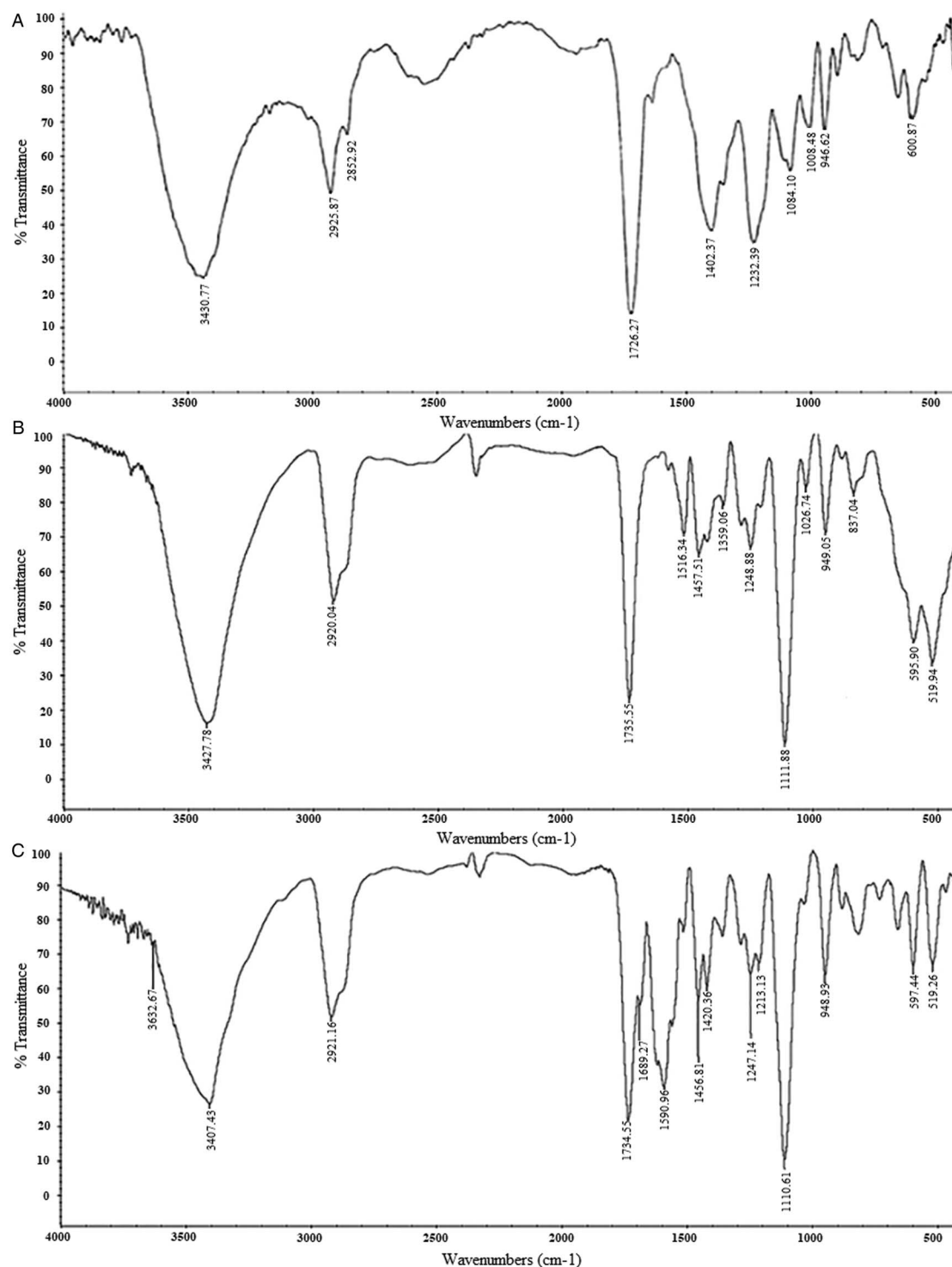


Fig. 5. FTIR spectra of ND (A), NDC (B) and NDC-CQ (C). The distinct peaks for each compound are shown. As the picture shows, CQ is loaded into NDC-CQ.

supernatant was removed, and parasites were isolated by adding 40 times the volume of 0.02% saponin in PBS 1 \times . The solution was then kept on ice for 30 min before it was centrifuged at 4 $^{\circ}$ C for 20 min at 2057 $\times g$ and washed three times with PBS 1 \times . The purified sedimented parasite was centrifuged at 25 200 $\times g$ at 4 $^{\circ}$ C for 5 min and the supernatant was removed (Parvazi *et al.*, 2016).

Parasite metabolites extraction

A total of 3 mL of physiological serum (0.9%) was added to the falcon tube containing purified parasites before homogenizing the sample with 9 KHz for 5 min using sonification. The sample

was then centrifuged for 10 min at 12 857 $\times g$. 200 μ L of cold 1.8 mM perchloric acid was added to the plate for every 10 8 parasites. The fluid pH was then adjusted and maintained at 6.8 by adding 5.4 M KOH. To induce acid sedimentation, the liquid was kept in ice for 60 min before centrifuging at 12 857 $\times g$ for 10 min and lyophilized. Finally, 1 mL D $_2$ O was added to the remaining powder to prepare the sample for NMR spectrophotometry (Parvazi *et al.*, 2016).

1H NMR spectra analysis

The spectra were directly entered into ProMetab in MATLAB software and were processed into a proper format for statistical

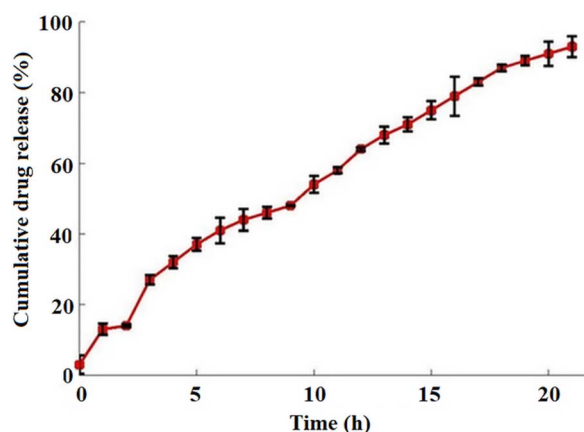


Fig. 6. The cumulative release curve of NDC-CQ from NDC. As the graph shows, the pattern of drug-release from nanoparticles follows the slow release pattern.

analysis. Spectra of each sample was divided into 1624 segments between 0 to 10 ppm chemical shifts and the peak attributed to water at 7.4 ppm was also removed. They were then converted to Excel files which were then entered into Metabo-Analyst website and analysed by partial least square-discriminate analysis. Differentiating metabolites were identified from their chemical shifts by the loading plots using the Human Metabolome Database. These identified metabolites were then entered into the MetaboAnalyst website using pathway analysis and biochemical pathways involved in the antimalarial properties of nanocomposites were identified.

Statistical analysis

After evaluation of data and confirming their normal distribution, the data were statistically analysed using SPSS V. 18 by one-way ANOVA, Student's *t*-test and nonlinear regression (sigmoidal dose-response model). *P* values <0.05 were considered statistically significant.

Results

The results of the nanocomposite characterization

Investigation of the size and weight of the synthesized nanoparticles using DLS and SLS revealed that the synthesized NDC with a size range of 90 nm, as a drug carrier for drug delivery into cells, and also the synthesized NDC-CQ with a size of 239 nm have suitable and acceptable sizes for the present study (Fig. 1). The molecular weight of NDC-CQ (kDa) by using the SLS method was reported on average 31.7 ± 3.02 . The SEM also confirmed DLS results (Fig. 2).

Liquid chromatography-mass spectrometry (LC-MS)

LC-MS was used to confirm the nanodendrimer G2 (Fig. 3). The peaks at 569 and 652 m/z^{-1} in the figure represent 8 and 9 repeating units (CH_2-CH_2-O , $M_w = 4$) of PEG with a citric acid group, respectively. There is also a 44-unite difference between other breaks. The difference is equal to the molecular weight of each CH_2-CH_2-O repeating unit of PEG molecule in the nano dendrimer G2.

Confirmation of covalent conjugation of nanodendrimers to curcumin

1H NMR spectroscopy was used to confirm the nanodendrimer-curcumin conjugate (NDC) as a nanocarrier. There were

simultaneously two binary peaks in the region of 2.5–3.5 ppm that these peaks indicated the presence of citric acid. In addition, a hydrogen peak and curvature in the regions of 3.8 and 5.5 ppm indicated the presence of polyethylene glycol in the composition and also the synthesis of the dendrimer G2. The presence of curcumin and covalent conjugation of nanodendrimer to curcumin were confirmed by peaks in the region of 7.6–6.6 ppm (Fig. 4).

Fourier-transform infrared (FTIR) spectroscopy

To confirm the structure of the synthesized nanocomposite (NDC-CQ), FTIR spectra were taken from different stages of synthesis. The peak at 2925 cm^{-1} belonged to the ester carbonyl group ($-CO-$) confirmed the synthesis of the dendrimer G2. Also, the presence of the peak belonging to the ester bond in the curcumin-dendrimer conjugate and the peaks belonging to dendrimer G2 and curcumin confirmed the conjugation (NDC). Broader absorbance peaks at $1590-1700\text{ cm}^{-1}$ clearly indicate that CQ was loaded into NCD (Fig. 5).

Drug-loading efficiency

According to the standard chart of CQ and curcumin (Supplementary Fig. 1), drug-loading efficiency for the synthesized NDC-CQ was estimated to be 87%.

Drug release study

The results of the drug release study at 7.4 pH showed a controlled drug-release pattern for the synthesized NDC-CQ, so that 92% of loaded drug was released within 48 h (Fig. 6).

Solubility and cellular uptake of the synthesized nanocomposite

The highest absorbance (400 nm) was obtained by spectrophotometry and according to the obtained results, the solubility of free curcumin, CQ and NDC-CQ was estimated to be 1, 71 and 92%, respectively. Therefore, the synthesized nanocomposite significantly increased the solubility of curcumin and CQ in water ($P < 0.05$). FCM results showed that fluorescence intensity of cells exposed to higher concentration of the nanocomposite was significantly higher than that of free curcumin and with increasing drug-exposure times, the rate of drug entry into the cell increased (Fig. 7).

Cytotoxicity activity

The results of the MTT assay on Vero cells are shown in Fig. 8. According to the diagram above, the toxicity of the synthesized NDC-CQ is 36% lower than that of CQ. The 50% cytotoxic concentration (CC_{50}) of NDC-CQ was observed at a concentration of $70\text{ }\mu\text{g mL}^{-1}$, which was much higher than the concentration needed to inhibit the growth of *P. falciparum* (IC_{50} : $1.52\text{ }\mu\text{g mL}^{-1}$) in the present study. Therefore, the synthesized nanocomposite at therapeutic dose had no toxic effect on Vero cells.

Effects of nanocomposite on the lysis of human RBCs

The synthesized nanocomposite at the therapeutic dose had no hemolytic effect on the human erythrocytes used for culture of *P. falciparum* parasite (Supplementary Fig. 2).

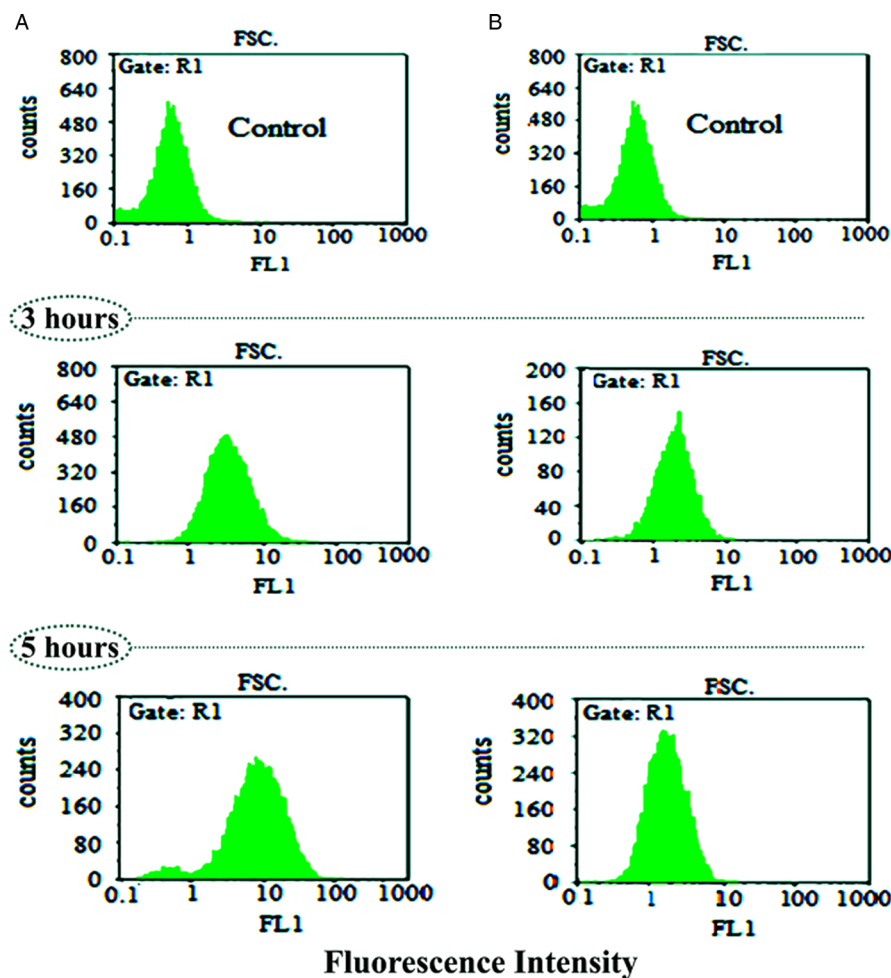


Fig. 7. Evaluation of cellular uptake of NDC-CQ (A) and curcumin as a control (B) at different times by FCM.

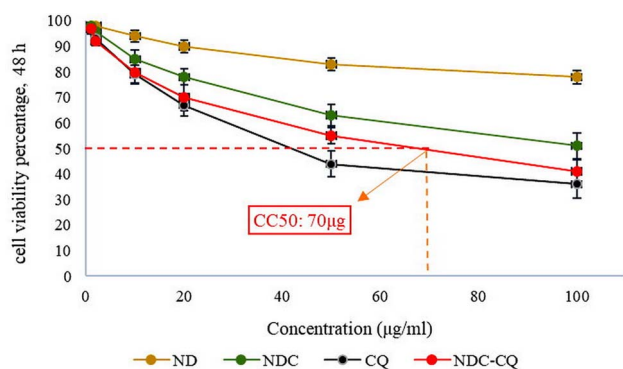


Fig. 8. Percentage of survival of Vero cells exposed to synthesized NDC-CQ compared to CQ and the control group within 48 h. The viability effects showed that $20 \mu\text{g mL}^{-1}$ NDC-CQ and NDC were perfectly nontoxic on the Vero cells compared with the control group. The values are expressed as mean \pm standard deviation from three independent experiments with $P < 0.001$.

Antiplasmodial activity of the nanocomposite

In order to evaluate the effect of the synthesized nanocomposite on *P. falciparum* parasite in culture medium, the number of live parasites in the medium was determined by microscopic and enzymatic methods (pFLDH). Analysis of the results showed that there was no significant difference between the above two methods in recording the results ($P > 0.05$). The number of *P. falciparum* parasites in the control group (placebo) was increased after 48-h incubation at 37°C (Table 1). Examination of microplate wells showed that the greatest cytotoxic effect of

the NDC-CQ was at $2.5 \mu\text{g}$ concentration, which was able to eliminate 82.6% of the parasites compared to the control group. Whereas the cytotoxic effect of CQ at this concentration ($2.5 \mu\text{g}$) was 55%, that this difference was statistically significant ($P < 0.05$) (Table 1). According to the results presented in Table 1, the synthesized NDC-CQ had more inhibitory effect on *P. falciparum* parasites than the CQ and curcumin alone. Nonlinear regression was used to obtain the IC_{50} value of the synthesized nanocomposite using the obtained results, the IC_{50} value of the nanocomposite was $1.52 \mu\text{g mL}^{-1}$ (Supplementary Fig. 3).

Metabolomics of *P. falciparum* in the presence of nanocomposite

The ^1H NMR spectra of metabolites of *P. falciparum* ring stages in the testing groups compared with control groups are shown in Fig. 9. The analysis of the data showed that there was a significant difference between metabolites, of *P. falciparum* ring stages, in the control group and the group receiving nanocomposite. These changes were mainly in the metabolic pathways of pyrimidine, TCA cycle, glutathione metabolism, aminoacyl-tRNA biosynthesis and glyoxylate and dicarboxylate metabolism (Table 2). Metabolic changes of the parasites exposed to CQ, as drug control, are listed in Fig. 14. Comparison of the obtained results showed that the metabolites of flavin mononucleotide, L-tyrosine and L-glutamine were changed only in the group receiving NDC-CQ, whereas in the group receiving CQ, these metabolites were unchanged. Therefore, 12 and 8 new metabolic pathways were induced, in *P. falciparum*, in the group receiving

Table 1. The growth inhibition percentage of *P. falciparum* in different groups, *in vitro*

Drug	Concentration ($\mu\text{g mL}^{-1}$)	Growth inhibition percentage			IC ₅₀ ($\mu\text{g mL}^{-1}$)
		Mic test \pm s.d.	pfLDH \pm s.d.	P value*	
NDC-CQ	0.1	11 \pm 1.8 ^d	8.1 \pm 1.4 ^d	0.125	1.52
	0.5	16.5 \pm 0.8 ^e	14.6 \pm 1.5 ^e	0.095	
	1	30.8 \pm 1.2 ^g	31.8 \pm 0.7 ^g	0.508	
	1.5	45.3 \pm 3 ^h	46.3 \pm 1.5 ^h	0.065	
	2	68.8 \pm 1.7 ⁱ	70.8 \pm 1.1 ⁱ	0.182	
	2.5	82.5 \pm 1.5 ^k	82.6 \pm 0.7 ^k	0.841	
NDC	1.5	2.8 \pm 0.7 ^{bc}	5.1 \pm 0.5 ^{bc}	0.074	9.06
	2	7 \pm 0.5 ^{cd}	7.6 \pm 0.7 ^{cd}	0.254	
	2.5	14.6 \pm 1.6 ^{ef}	15.5 \pm 0.5 ^{ef}	0.457	
CQ	1.5	17.8 \pm 1.2 ^f	17.3 \pm 0.2 ^f	0.653	2.31
	2	35.8 \pm 1 ^g	33.8 \pm 0.7 ^g	0.345	
	2.5	53.8 \pm 2.8 ^m	55.6 \pm 1.5 ^m	0.401	
Curcumin	2.5	2.5 \pm 0.5 ^{ab}	3 \pm 0.5 ^{ab}	0.288	
ND	2.5	0 ^a	0 ^a	–	
DV	–	0 ^a	0.3 \pm 0.3 ^a	0.158	
Control	–	0 ^a	0 ^a	–	

The similar letter in the table indicates that there is no significant relationship between the groups ($P > 0.05$).

*The difference between the microscopic and enzymatic (pfLDH) methods (the statistics were regarded significant at $P < 0.05$).

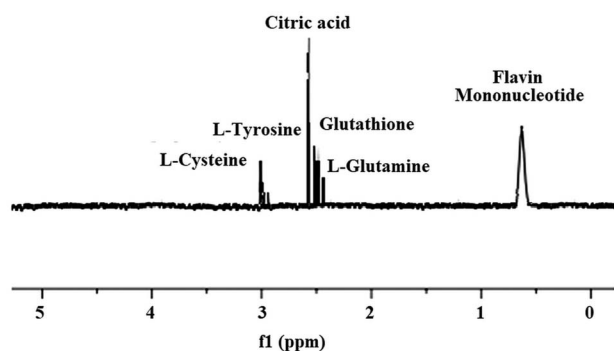


Fig. 9. Superimposed spectra of NDC-CQ treated *P. falciparum*.

NDC-CQ compared to the control group and compared to the group receiving CQ (drug control), respectively (Figs 10–12).

This shows the detailed results from the pathway analysis using over representation analysis with the hypergeometric test. Since many pathways are tested at the same time, the statistical P values from enrichment analysis are further adjusted for multiple testings. The total/maximum importance of each pathway is 1; the importance measure of each metabolite node is actually the percentage w.r.t the total pathway importance, and the pathway impact value is the cumulative percentage from the matched metabolite nodes. In the table the column named as Total is the total number of compounds in the pathway; the Hits are the actually matched number from the user uploaded data; the Raw P is the original P value calculated from the enrichment analysis; the impact is the pathway impact value calculated from pathway topology analysis. In Fig. 13 the circles higher, bigger and closer to the y axis are of greater importance. Metabolic changes of the parasites exposed to NDC-CQ are listed in Table 3 (Namazi and Adeli, 2003).

Discussion

The method used to synthesize PEG dendrimers in previous studies was time consuming and costly and in addition, toxic substances such as dichloromethane and pyridine were used in its synthesis (Namazi and Adeli, 2003; Namazi and Adeli, 2005). However, in the present study, a new method was used to synthesize nano-PEG, which in addition to using substances with very low toxicity such as DCC and EDC as activators, instead of using dichloromethane and pyridine toxicants, the reaction time and also the time to reach the product were significantly reduced.

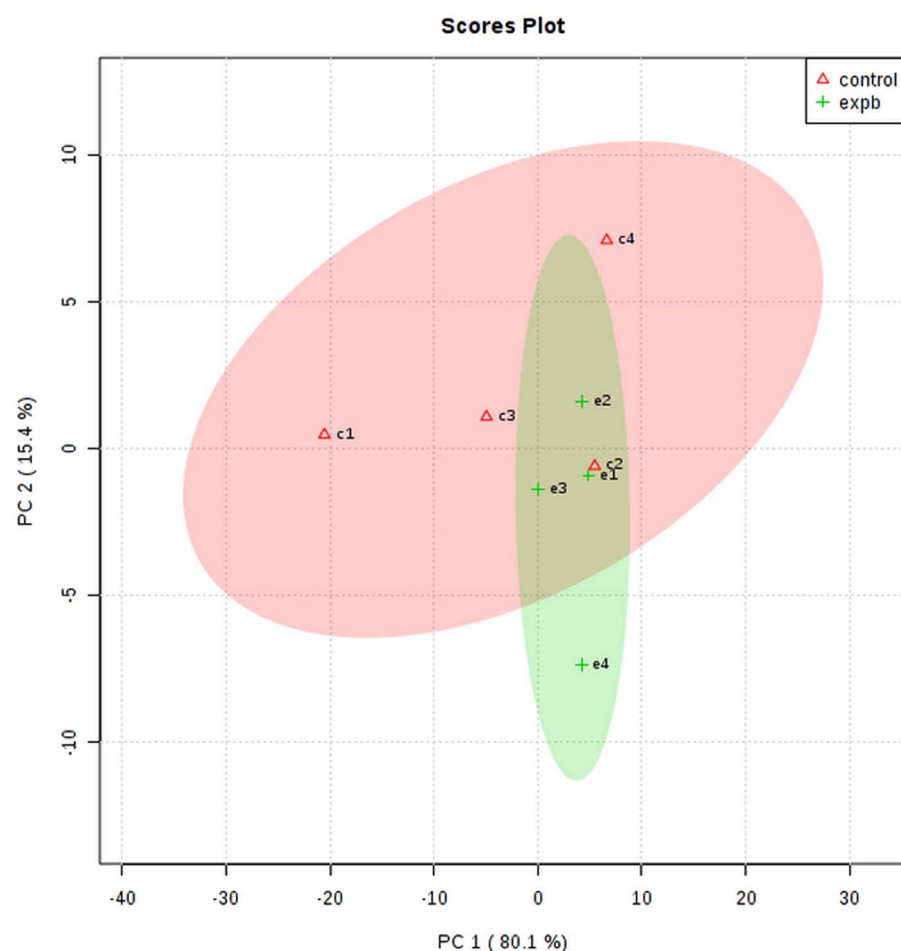
Jafari Iri Sofla *et al.* (2015) showed that poly(amidoamine) dendrimers (PAMAM), at a concentration of $1000 \mu\text{g mL}^{-1}$, were toxic to BT-474 cells and Hung *et al.* (2011) found that unmodified poly(amidoamine) dendrimers cause pores in cell membranes and cell death. The results of a study showed that the G2 dendrimer was less toxic to MCF-7 cells than other dendrimer generations (G1, G3 and G4) (Pan *et al.*, 2007). The MTT results of the present study also confirmed the non-toxicity of this dendrimer and indicated that the synthesized nano-carrier had/has no toxicity to Vero cells up to high concentrations ($100 \mu\text{g mL}^{-1}$).

The solubility and biological activity of curcumin and chloroquine in water increased with the help of nanocarriers used in this study. According to the study by Alavidjeh *et al.* (2010), PEG, which is the core of this dendrimer, is not only fully biocompatible but also highly water soluble. This polyether compound, with citric acid side branches which have a negative charge, is not toxic to cell and is completely soluble in water. These nanocarriers, in addition to solubilizing the drug in water, protect the curcumin and chloroquine by further stabilizing the drug against degradation, which is consistent with the study by Erfani-Moghadam *et al.* (2014). When the biodegradability of these dendrimers was studied by Alavidjeh *et al.*, they found that second-generation dendrimers (G2), under enzymatic conditions, are biodegradable

Table 2. Differentiating metabolites and pathways in the control and treated *P. falciparum* with IC₅₀ dose of CQ and NDC-CQ

No.	Metabolic pathways	NDC-CQ/CQ	Total	Expected	Hits	Raw <i>P</i>	Impact
1	Glyoxylate and dicarboxylate metabolism	+/+	12	0.27	2	2.62×10^{-2}	0.50
2	Nitrogen metabolism	+/-	3	0.07	1	6.55×10^{-2}	0.00
3	Riboflavin metabolism	+/-	3	0.07	1	6.55×10^{-2}	1.00
4	Aminoacyl-tRNA biosynthesis	+/-	46	1.02	3	7.23×10^{-2}	0.00
5	Glutathione metabolism	+/+	21	0.47	2	7.48×10^{-2}	0.39
6	Phenylalanine, tyrosine and tryptophan biosynthesis	+/-	6	0.13	1	1.27×10^{-1}	0.01
7	Thiamine metabolism	+/+	11	0.24	1	2.22×10^{-1}	0.02
8	Alanine, aspartate and glutamate metabolism	+/-	12	0.27	1	2.39×10^{-1}	0.26
9	Cysteine and methionine metabolism	+/-	14	0.31	1	2.74×10^{-1}	0.00
10	Arginine and proline metabolism	+/-	17	0.38	1	3.23×10^{-1}	0.00
11	Citrate cycle (TCA cycle)	+/+	20	0.45	1	3.69×10^{-1}	0.13
12	Pyrimidine metabolism	+/-	31	0.69	1	5.15×10^{-1}	0.03
13	Terpenoid backbone biosynthesis	-/+	15	0.20	1	1.85×10^{-1}	0.00
14	Pyruvate metabolism	-/+	20	0.27	1	2.40×10^{-1}	0.15
15	Glycolysis or Gluconeogenesis	-/+	23	0.31	1	2.72×10^{-1}	0.10

Total, total number of compounds in the pathway; Hits, the actual matched number from data uploaded by user; Raw *P*, the *P* value derived from enrichment analysis; Holm *P*, the *P* value adjusted using Holm–Bonferroni method; FDR *P*, the *P* value adjusted using false discovery rate; Impact, the pathway impact value derived by pathway topology analysis. The table above incorporates the detailed results from pathway analysis. The statistical *P* values from enrichment analysis are further adjusted for multiple testing to accommodate for many pathways that are tested simultaneously.

**Fig. 10.** PLS-DA scores plot showing the separation of two groups (the control group and test group receiving the IC₅₀ dose of NDC-CQ).

in the cell and can be metabolized and excreted by other cell processes (Alavidjeh *et al.*, 2010).

The adsorption kinetics studies of the nanocomposite using FCM and fluorescence microscopy are possible due to the

intrinsic fluorescence characteristics of curcumin. In the present study, due to the presence of curcumin–dendrimer conjugate in the synthesized nanocomposite, a 4-fold increase in the cellular uptake of curcumin was observed (80% cellular uptake of

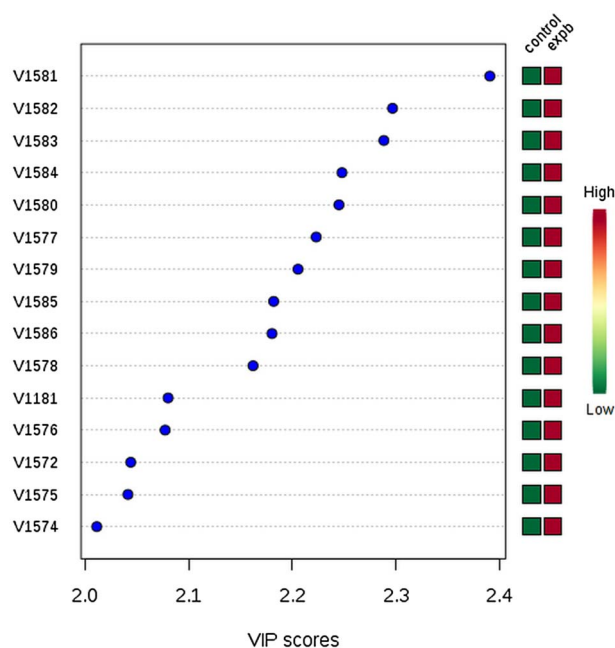


Fig. 11. Important features identified by PLS-DA. In VIP scores, the chemical shifts of the metabolites in the test group are shown in green (a decrease in metabolites) and red (an increase in metabolites).

curcumin conjugate in the composite compared with 20% cellular uptake of free curcumin). This increase in uptake appears to be due to the increased solubility of curcumin, due to the presence of dendrimer, and dendrimer entry into the cell by endocytosis, as for other nanoparticles also, the involvement of endocytosis in cellular uptake has been identified (Sahu *et al.*, 2008). Also, the results of the present study showed that the cellular uptake of the nanocomposite was time dependent. Babaei *et al.* (2012) have also reported a time-dependent cell uptake of dendrosomal nanocurcumin.

One of the problems of using drug–nanocarrier conjugates is the rapid release of drug and elimination of the drug before reaching the target tissue, but in the present study, the synthesized nanocomposite showed slow release behaviour and provided longer-term protection for the drug. Given that combination therapies are now used to treat a variety of diseases, including malaria, and according to the WHO recommendation of using natural herbal medicines which can be useful and more effective due to its lower side-effects (Elmi *et al.*, 2014). Therefore, in the present study, curcumin was used as a natural compound for the preparation of the NDC conjugate and to increase the effect of the synthesized nanocomposite, chloroquine was loaded into the complex (NDC-CQ) as a novel antimalarial drug. In the studies by Cui *et al.* (2007) and Reddy *et al.* (2005) IC_{50} values of curcumin on *P. falciparum* *in vitro* (culture medium) were reported 24.69 ± 0.47 and $5 \mu M$, respectively. However, in the present study, IC_{50} values for curcumin alone and for curcumin conjugated to the G2 dendrimer (NDC) were 12 and $9 \mu g mL^{-1}$ (32 and $24 \mu M$), respectively. Therefore, nanodendrimer G2 has increased the effect of curcumin on *Plasmodium* parasite, by increasing the solubility of curcumin, which confirms the study by Debnath *et al.* (2013) in this study they showed that the dendrimer increased the solubility of curcumin and also its anticancer activity. Many investigations have been performed around the world on different nanocarriers and nanodrugs to achieve the suitable drug in the fight against malaria including the study by Panneerselvam *et al.* (2011). The results from this study showed that the synthesized silver nanoparticles at a concentration of $100 \mu g mL^{-1}$ removed 83% of *P. falciparum* parasites. By

nanosizing decoquinatate, Wang *et al.*, (2014) were able to reduce its effective dose rate on hepatic forms of *P. berghei* (from 20 to $1.25 mg kg^{-1}$), which led to a decrease in drug toxicity. According to Jawetz law on antimicrobial combination, the combination of two drugs may have synergistic, additive or antagonistic effects (Sonne and Jawetz, 1969). The results of study by Oyeyemi *et al.* (2018) showed that the combination of curcumin and artemisinin has a synergistic effect.

The results of the present study also showed that chloroquine, as a drug to treat malaria, with NDC, as a natural herbal compound, had a better effect than the drugs alone, so that the obtained NDC-CQ at a concentration of $2.5 \mu g mL^{-1}$ prevented the growth of *P. falciparum* parasites (82.6%) in the culture medium, which was more than the sum of inhibitory effects of chloroquine (55.6%) and curcumin (15.5%) alone. Therefore, the effect of chloroquine and curcumin together on the nanocomposite is greater than the effect of chloroquine and curcumin alone, which may be due to the synergistic effect of these two compounds on each other.

In study by Neto *et al.* (2013), which is consistent with our study, the results showed that the use of antimalarial drugs combined with curcumin is more effective than the use of these drugs alone.

In the present study, the metabolic cycles of parasite before and after exposure to NDC-CQ were investigated by the 1H NMR method, for the exact evaluation of the effect of the synthesized nanocomposite on plasmodium parasites. The metabolites and altered metabolic pathways, in the present study, are presented in Tables 2 and 3.

The results showed that the metabolic cycle of glyoxylate and dicarboxylate exhibited the greatest change compared to the control group, which is consistent with the study by Han *et al.* (2009) on artemisinin. Therefore, synthesized NDC-CQ and artemisinin affect the common metabolic cycle, which may indicate the similar effects of the two drugs, which of course, needs further investigation.

In the present study, the metabolites of L-glutamine were affected by the metabolic pathway of glyoxylate and dicarboxylate. Various studies have shown that in *Plasmodium*-infected red blood cells, glutamine is converted to glutamate, that the reaction is catalysed by glutaminase and 7-glutamyl-transpeptidase. According to the study by Elford *et al.* (1985), the glutamine level can be associated with the lysis of erythrocytes by the parasite. Our study also showed an increase in the amount of glutamine compared to the control group, which is consistent with the above study. On the other hand, according to a study, the amount of glutamine is effective in invasion of red blood cells by parasites (Vilmont *et al.*, 1990).

Another altered metabolic pathway in the present study was nitrogen metabolism which, like glyoxylate and dicarboxylate metabolism pathways, altered the metabolism of L-glutamine. The third altered metabolic pathway was riboflavin metabolism. The study by Akompong *et al.* (2000) showed that the riboflavin cycle is involved in asexual development and production of food vacuoles of *P. falciparum*. The results of their study showed that riboflavin plays a role in the production of hemozoin and the rate of haemoglobin consumption by the parasite. Therefore, it could be a suitable drug target in the future to combat malaria caused by *P. falciparum*.

A study, by Parvazi *et al.* (2016) on cinnamon extract showed that it leads to changes of succinic acid, glutathione and β -alanine metabolites in the parasite extract, which was not seen in our study. This could be due to the fact that the nanodendrimer contained both CQ and curcumin whereas Parvazi *et al.* had used cinnamon extract alone and therefore, the differences in the metabolic cycle obtained from the study by Parvazi *et al.*, and the

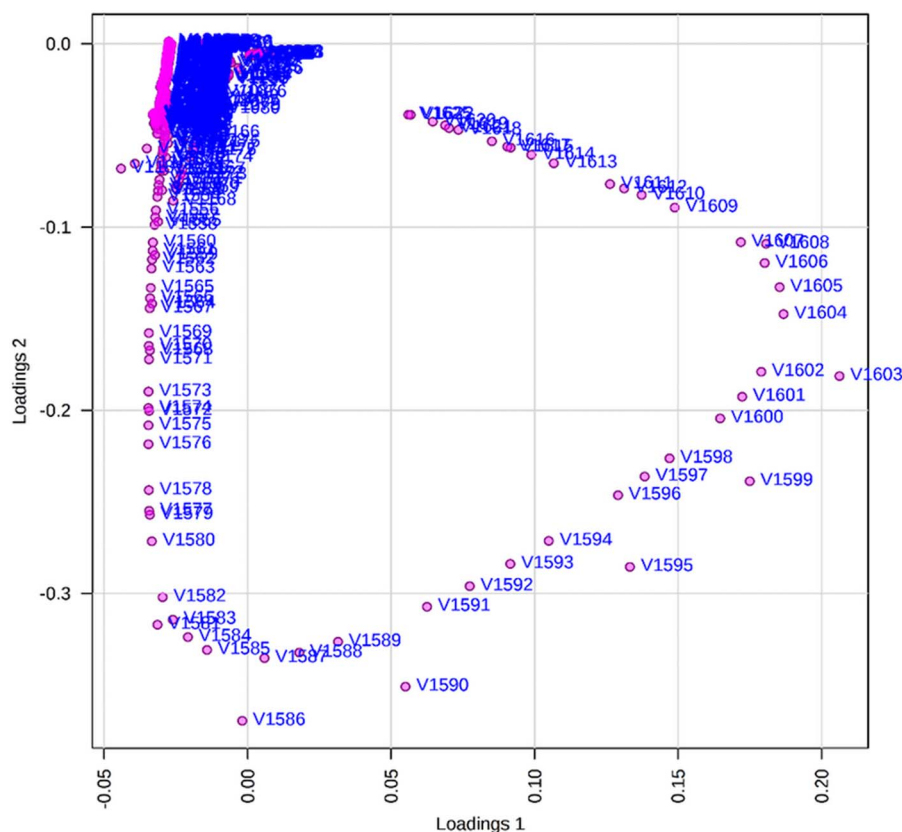


Fig. 12. Loadings plot for the selected PCs. In the loading plot the categorization of the two control and test groups is indicated by deleting the low value data, without changing the original meaning of the data. The chemical shift of the metabolites, that has the most changes relative to the centre of the plot, is determined.

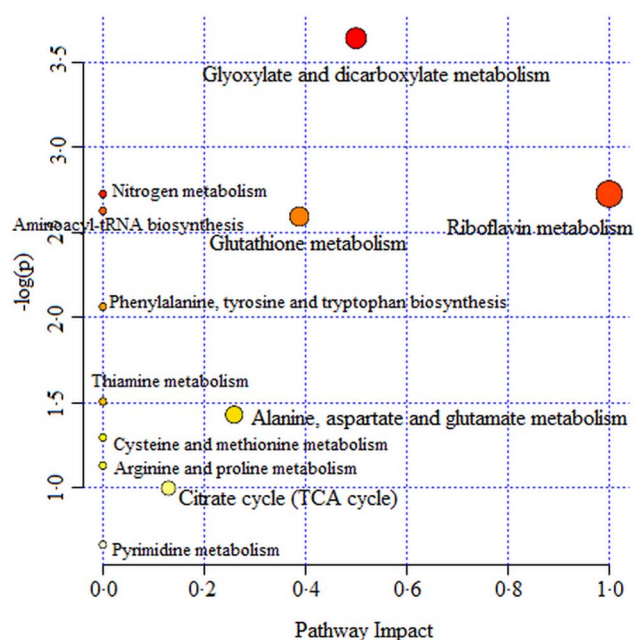


Fig. 13. Pathway analysis of the groups receiving NDC-CQ. Pathway analysis showing all matched pathways according to *P* values from pathway enrichment analysis and pathway impact values from pathway topology analysis.

present study may be due to differences in the nature of the drugs used in these two studies.

Another metabolic pathway modified by synthesized NDC-CQ was aminoacyl-tRNA biosynthesis. According to the study of Nyamai and Tastan Bishop (2019), this metabolic pathway in addition to synthesizing the first enzyme required for protein translation and amino acid catalysis, is different in humans and the parasite *Plasmodium*. Therefore, it is considered as a suitable

Table 3. Metabolites with their chemical shifts were identified from HMDB

No.	Metabolite name	Chemical shift	HMDB No.	Flux
1	Flavin mononucleotide	0.6375	HMDB0001520	↑
2	L-glutamine	2.5275	HMDB0000641	↑
3	L-cysteine	3.0275	HMDB0000574	↑
4	Citric acid	2.5525	HMDB0000094	↑
5	Glutathione	2.5375	HMDB0000125	↑
6	L-tyrosine	2.9875	HMDB0000158	↑

drug target for antimalarial drug development. The nucleus of *P. falciparum* has two codes for methionyl tRNA synthetase, which are called pfmrscy and pfmrspi. For many years, this enzyme has been known as a target for anti-bacterial, anti-fungal drugs.

In recent years, many investigations have been carried out on this enzyme, as a drug target, in eukaryotes (Hussain *et al.*, 2015), because of the importance of this topic, James *et al.* investigated the synthesis of amino-acyl tRNA in eukaryotic parasites (Turner *et al.*, 2006). Since the parasitic t-RNA synthetase has a soluble crystalline structure, it can be a suitable target for anti-parasitic drugs, including drugs against *P. falciparum* malaria (Pham *et al.*, 2013). In the future, it is hoped that this enzyme may be used as a target for anti-parasitic drugs.

Another important metabolic cycle that changed in the present study was the TCA cycle.

The study by Ginsburg (2010) showed that the blood stage of the parasite requires the TCA cycle, for glucose fermentation to produce energy, and has the enzymes needed for this cycle. The results of the study by Olszewski *et al.* (2010) showed that the metabolism of the Krebs cycle in *P. falciparum* is greatly separated from glycolysis. The main carbon sources for the Krebs cycle are

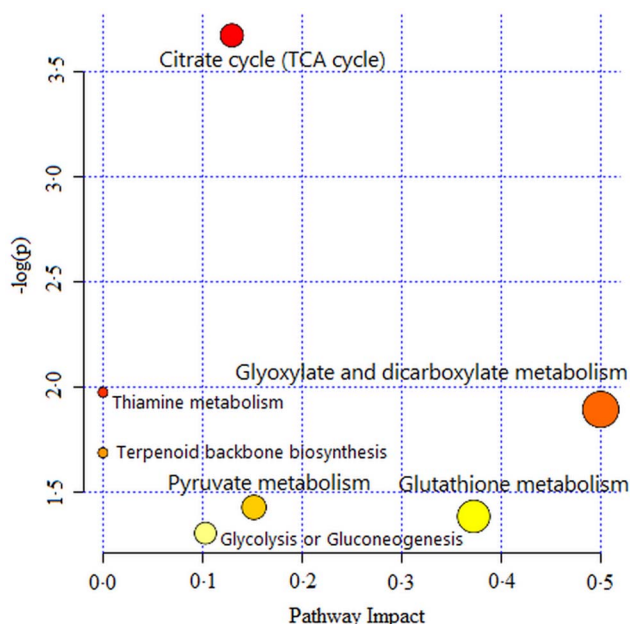


Fig. 14. Pathway analysis of the groups receiving CQ.

aspartate, asparagine, glutamate and glutamine amino acids, which are created by the breakdown of the haemoglobin molecule, are then deaminated and converted to oxaloacetate or alpha ketoglutarate. They believed that the Krebs cycle in the parasite *P. falciparum* is not like a cycle but rather has a branched structure with several reactions which act in the opposite direction of the standard pathway of the Krebs cycle (Olszewski *et al.*, 2010), but this theory has been rejected (Olszewski and Llinas, 2011).

The NDC-CQ compared with the negative control group caused metabolic changes in pathways, as shown in Table 2. Changes in some metabolic pathways, such as glyoxylate, dicarboxylate, glutathione, thiamine and citrate cycles (TCA cycles), were observed in the NDC-CQ and drug control group (CQ) (Fig. 14). Due to the use of CQ in the NDC-CQ, the obtained results were consistent with predictions. The alterations in the metabolic pathways (terpenoid backbone biosynthesis, pyruvate metabolism and glycolysis or gluconeogenesis) in the CQ recipient group and not altering of these metabolic pathways in the NDC-CQ group were on the other hand unexpected. Due to the use of CQ in the structure of the NDC-CQ, it was expected that all of the metabolic pathways of the CQ group would also be altered in the NDC-CQ group. However, the investigation of altered metabolites in these pathways revealed that only pyruvic acid metabolite was affected by the mentioned pathways. Since pyruvic acid has been altered by other pathways, such as the metabolism of thiamine and the citrate cycle (TCA cycle), therefore the NDC-CQ, similar to CQ, has led to changes in pyruvic acid metabolite but from other metabolic pathways.

In this study, ¹H NMR spectroscopy was used with untargeted metabolomics to study the effect of the nanocomposite on *P. falciparum* *in vitro*. Targeted metabolomics using LC-MS would help deepen the understanding about the drug targets effected by the nanocomposite, by identification of drug targets and by allowing detailed characterization of modes of action and resistance of existing and novel antiprotozoal drugs. The metabolic pathways altered by the synthesized nanocomposite were different from the ones exhibited by other drugs.

Conclusion

With regard to the better effect of the synthesized nanodrug on *P. falciparum* in the culture medium compared to CQ, this

nanodrug can be considered as an effective anti-*Plasmodium* compound that more comprehensive research studies in this area are recommended. On the other hand, a more thorough review of metabolites for understanding the life cycle of malaria parasites in the host may be helpful, because it will lead to the identification of effective pathways and metabolites induced by the drug (drug intended to prevent malaria) and also reveal the involvement of new interveners in the fight against malaria.

Supplementary material. The supplementary material for this article can be found at <https://doi.org/10.1017/S0031182020000372>.

Acknowledgements. The authors would like to thank the Pasteur Institute of Iran for carrying out the *in vitro* studies involving the culture of *P. falciparum*.

Financial support. The authors would like to thank the Iran University of Medical Sciences for providing the necessary funding for this research.

Conflicts of interest. The authors declare that they have no conflicts of interest.

Ethical standards. Performing the procedures required for the study was approved by the Ethical Committee of the Faculty of Medicine (Iran University of Medical Sciences). The code of: IR.IUMS.FMD.REC.1396.9321577004 was designated for the study which was in accordance with the Declaration and Guidelines.

References

- Abbasi E, Aval SF, Akbarzadeh A, Milani M, Nasrabadi HT, Joo SW, Hanifehpour Y, Nejati-Koshki K and Pashaei-Asl R (2014) Dendrimers: synthesis, applications, and properties. *Nanoscale Research Letters* **9**, 247.
- Akompong T, Ghorri N and Haldar K (2000) In vitro activity of riboflavin against the human malaria parasite *Plasmodium falciparum*. *Antimicrobial Agents and Chemotherapy* **44**, 88–96.
- Alavidjeh MS, Haririan I, Khorramzadeh MR, Ghane ZZ, Ardestani MS and Namazi H (2010) Anionic linear-globular dendrimers: biocompatible hybrid materials with potential uses in nanomedicine. *Journal of Materials Science. Materials in Medicine* **21**, 1121–1133.
- Antinori S, Galimberti L, Milazzo L and Corbellino M (2012) Biology of human malaria plasmodia including *Plasmodium knowlesi*. *Mediterranean Journal of Hematology and Infectious Diseases* **4**, e2012013–e2012013.
- Babaei E, Sadeghizadeh M, Hassan ZM, Feizi MA, Najafi F and Hashemi SM (2012) Dendrosomal curcumin significantly suppresses cancer cell proliferation in vitro and in vivo. *International Immunopharmacology* **12**, 226–234.
- Braga CBE, Martins AC, Cayotopa ADE, Klein WW, Schlosser AR, da Silva AF, de Souza MN, Andrade BWB, Filgueira-Júnior JA, Pinto WDJ and da Silva-Nunes M (2015) Side effects of chloroquine and primaquine and symptom reduction in malaria endemic area (Mâncio Lima, Acre, Brazil). *Interdisciplinary Perspectives on Infectious Diseases* **2015**, 346853–346853.
- Bruni N, Stella B, Giraud L, Della Pepa C, Gastaldi D and Dosio F (2017) Nanostructured delivery systems with improved leishmanicidal activity: a critical review. *International Journal of Nanomedicine* **12**, 5289–5311.
- Cui L, Miao J and Cui L (2007) Cytotoxic effect of curcumin on malaria parasite *Plasmodium falciparum*: inhibition of histone acetylation and generation of reactive oxygen species. *Antimicrobial Agents and Chemotherapy* **51**, 488–494.
- Debnath S, Salloum D, Dolai S, Sun C, Averick S, Raja K and Fata J (2013) Dendrimer-curcumin conjugate: a water soluble and effective cytotoxic agent against breast cancer cell lines. *Anti-Cancer Agents in Medicinal Chemistry* **13**, 1531–1539.
- Elford BC, Haynes JD, Chulay JD and Wilson RJ (1985) Selective stage-specific changes in the permeability to small hydrophilic solutes of human erythrocytes infected with *Plasmodium falciparum*. *Molecular and Biochemical Parasitology* **16**, 43–60.
- Elmi T, Gholami S, Azadbakht M and Ziaei H (2014) Effect of chloroformic extract of *Tanacetum parthenium* in the treatment of *Giardia lamblia* infection in Balb/c mice. *Journal of Mazandaran University of Medical Sciences* **23**, 157–165.

- Elmi T, Hajjaliani F, Asadi MR, Orujzadeh F, Kalantari Hesari A, Rahimi Esboei B and Gholami S (2019) A study on the effect of Zingiber Officinale hydroalcoholic extract on Plasmodium berghei in infected mice: an experimental study. *Journal of Rafsanjan University of Medical Sciences* **18**, 353–364.
- Erfani-Moghadam V, Nomani A, Najafi F, Yazdani Y and Sadeghzadeh M (2014) Design and synthesis of a novel dendrosome and a PEGylated PAMAM dendrimer nanocarrier to improve the anticancer effect of turmeric (*Curcuma longa*) curcumin. *Pathobiology Research* **17**, 63–77.
- Faye B, Ndiaye JL, Ndiaye D, Dieng Y, Faye O and Gaye O (2007) Efficacy and tolerability of four antimalarial combinations in the treatment of uncomplicated *Plasmodium falciparum* malaria in Senegal. *Malaria Journal* **6**, 80.
- Ghimire P, Singh N, Ortega L, Rijal KR, Adhikari B, Thakur GD and Marasini B (2017) Glucose-6-phosphate dehydrogenase deficiency in people living in malaria endemic districts of Nepal. *Malaria Journal* **16**, 214.
- Ginsburg H (2010) Malaria parasite stands out. *Nature* **466**, 702–703.
- Guo Z (2016) Artemisinin anti-malarial drugs in China. *Acta Pharmaceutica Sinica. B* **6**, 115–124.
- Han L, Huang Q, Nan P and Zhong Y (2009) Prediction of potential antimalarial targets of artemisinin based on protein information from whole genome of *Plasmodium falciparum*. *Chinese Science Bulletin* **54**, 4234.
- Haririan I, Alavidjeh MS, Khorramzadeh MR, Ardestani MS, Ghane ZZ and Namazi H (2010) Anionic linear-globular dendrimer-cis-platinum (II) conjugates promote cytotoxicity in vitro against different cancer cell lines. *International Journal of Nanomedicine* **5**, 63–75.
- Hung W-I, Hung C-B, Chang Y-H, Dai J-K, Li Y, He H, Chen S-W, Huang T-C, Wei Y, Jia X-R and Yeh J-M (2011) Synthesis and electroactive properties of poly(amidoamine) dendrimers with an aniline pentamer shell. *Journal of Materials Chemistry* **21**, 4581–4587.
- Hussain T, Yogavel M and Sharma A (2015) Inhibition of protein synthesis and malaria parasite development by drug targeting of methionyl-tRNA synthetases. *Antimicrobial Agents and Chemotherapy* **59**, 1856–1867.
- Jafari Iri Sofla F, Rahbarzadeh F and Ahmadvand D (2015) Evaluation of poly(amidoamine) dendrimer surface modification with poly(ethylene glycol) on cytotoxicity reduction. *Pathobiology Research* **18**, 23–38.
- Lazaro JE and Gay F (1998) *Plasmodium falciparum*: in vitro cytotoxicity testing using MTT. *Journal of Biomolecular Screening* **3**, 49–53.
- Lo ST, Kumar A, Hsieh JT and Sun X (2013) Dendrimer nanoscaffolds for potential theranostics of prostate cancer with a focus on radiochemistry. *Molecular Pharmaceutics* **10**, 793–812.
- Lu D-Y (2015) 6 – drug combinations. In Lu D-Y (ed.). *Personalized Cancer Chemotherapy*. Oxford: Woodhead Publishing, pp. 37–41.
- Makler MT and Hinrichs DJ (1993) Measurement of the lactate dehydrogenase activity of *Plasmodium falciparum* as an assessment of parasitemia. *American Journal of Tropical Medicine and Hygiene* **48**, 205–210.
- Mehrzi TZ, Ardestani MS, Molla Hoseini MH, Khamesipour A, Mosaffa N and Ramezani A (2018) Novel nano-sized chitosan amphotericin B formulation with considerable improvement against *Leishmania major*. *Nanomedicine (Lond)* **13**, 3129–3147.
- Memar B, Jamili S, Shahbazzadeh D and Bagheri KP (2016) The first report on coagulation and phospholipase A2 activities of Persian gulf lionfish, *Pterois russelli*, an Iranian venomous fish. *Toxicon* **113**, 25–31.
- Mukherjee R, Patra M, Dutta D, Banik M and Basu T (2016) Tetracycline-loaded calcium phosphate nanoparticle (Tet-CPNP): rejuvenation of an obsolete antibiotic to further action. *Biochimica et Biophysica Acta (BBA) – General Subjects* **1860**, 1929–1941.
- Namazi H and Adeli M (2003) Novel linear-globular thermoreversible hydrogel ABA type copolymers from dendritic citric acid as the A blocks and poly(ethyleneglycol) as the B block. *European Polymer Journal* **39**, 1491–1500.
- Namazi H and Adeli M (2005) Dendrimers of citric acid and poly(ethylene glycol) as the new drug-delivery agents. *Biomaterials* **26**, 1175–1183.
- Namazi H, Motamedi S and Namvari M (2011) Synthesis of new functionalized citric acid-based dendrimers as nanocarrier agents for drug delivery. *BioImpacts: BI* **1**, 63–69.
- Neto Z, Machado M, Lindeza A, do Rosário V, Gazarini ML and Lopes D (2013) Treatment of plasmodium chabaudi parasites with curcumin in combination with antimalarial drugs: drug interactions and implications on the ubiquitin/proteasome system. *Journal of Parasitology Research*, **2013**, 11.
- Nyamai DW and Tasthan Bishop Ö (2019) Aminoacyl tRNA synthetases as malarial drug targets: a comparative bioinformatics study. *Malaria Journal* **18**, 34.
- Olszewski KL and Llinas M (2011) Central carbon metabolism of plasmodium parasites. *Molecular and Biochemical Parasitology* **175**, 95–103.
- Olszewski KL, Mather MW, Morrisey JM, Garcia BA, Vaidya AB, Rabinowitz JD and Llinas M (2010) Branched tricarboxylic acid metabolism in *Plasmodium falciparum*. *Nature* **466**, 774.
- Oyeyemi O, Morenkeji O, Afolayan F, Dauda K, Busari Z, Meena J and Panda A (2018) Curcumin-artesunate based polymeric nanoparticle; anti-plasmodial and toxicological evaluation in murine model. *Frontiers in Pharmacology* **9**, 1–8.
- Pan B, Cui D, Xu P, Huang T, Li Q, He R and Gao F (2007) Cellular uptake enhancement of polyamidoamine dendrimer modified single walled carbon nanotubes.
- Panneerselvam C, Ponarulsevam S and Murugan K (2011) Potential anti-plasmodial activity of synthesized silver nanoparticle using *Andrographis paniculata* Nees (Acanthaceae). *Archives of Applied Science Research* **3**, 208–2017.
- Parvazi S, Sadeghi S, Azadi M, Mohammadi M, Arjmand M, Vahabi F, Sadeghzadeh S and Zamani Z (2016) The effect of aqueous extract of cinnamon on the metabolome of *Plasmodium falciparum* using ¹H NMR spectroscopy. *Journal of Tropical Medicine* **2016**, 5.
- Pham JS, Dawson KL, Jackson KE, Lim EE, Pasaje CFA, Turner KEC and Ralph SA (2013) Aminoacyl-tRNA synthetases as drug targets in eukaryotic parasites. *International Journal for Parasitology. Drugs and Drug Resistance* **4**, 1–13.
- Rahmani A, Alsahli M, Aly S, Khan M and Aldebasi Y (2018) Role of curcumin in disease prevention and treatment. *Advanced Biomedical Research* **7**, 38–38.
- Reddy RC, Vatsala PG, Keshamouni VG, Padmanaban G and Rangarajan PN (2005) Curcumin for malaria therapy. *Biochemical and Biophysical Research Communications* **326**, 472–474.
- Sahu A, Kasoju N and Bora U (2008) Fluorescence study of the curcumin-casein micelle complexation and its application as a drug nanocarrier to cancer cells. *Biomacromolecules* **9**, 2905–2912.
- Sonne M and Jawetz E (1969) Combined action of carbenicillin and gentamicin on *Pseudomonas aeruginosa* in vitro. *Applied Microbiology* **17**, 893–896.
- Tagbor H, Bruce J, Browne E, Randal A, Greenwood B and Chandramohan D (2006) Efficacy, safety, and tolerability of amodiaquine plus sulphadoxine-pyrimethamine used alone or in combination for malaria treatment in pregnancy: a randomised trial. *Lancet* **368**, 1349–1356.
- Tallarida RJ (2011) Quantitative methods for assessing drug synergism. *Genes & Cancer* **2**, 1003–1008.
- Tiwari B, Pahuja R, Kumar P, Rath SK, Gupta KC and Goyal N (2017) Nanotized curcumin and miltefosine, a potential combination for treatment of experimental visceral leishmaniasis. *Antimicrobial Agents and Chemotherapy* **61**, 01169–16.
- Trager W and Jensen JB (1976) Human malaria parasites in continuous culture. *Science (New York, N.Y.)* **193**, 673–675.
- Turner J, Graziano J, Spraggon G and Schultz P (2006) Structural plasticity of an aminoacyl-tRNA synthetase active site. *Proceedings of the National Academy of Sciences of the USA* **103**, 6483–6488.
- Tyagi P, Singh M, Kumari H, Kumari A and Mukhopadhyay K (2015) Bactericidal activity of curcumin I is associated with damaging of bacterial membrane. *PLoS ONE* **10**, e0121313.
- Vilmont M, Azoulay M and Frappier F (1990) Metabolism of glutamine in erythrocytes infected with the human malaria parasite: *Plasmodium falciparum*. *Annales de Parasitologie Humaine et Comparee* **65**, 162–166.
- Wang H, Li Q, Reyes S, Zhang J, Zeng Q, Zhang P, Xie L, Lee PJ, Roncal N, Melendez V, Hickman M and Kozar MP (2014) Nanoparticle formulations of decoquinone increase antimalarial efficacy against liver stage plasmodium infections in mice. *Nanomedicine: Nanotechnology, Biology, and Medicine* **10**, 57–65.
- WHO (2019) World malaria report 2019. Licence: CC BY-NC-SA 3.0 IGO, 1–232.
- Zia Q, Mohammad O, Rauf MA, Khan W and Zubair S (2017) Biomimetically engineered amphotericin B nano-aggregates circumvent toxicity constraints and treat systemic fungal infection in experimental animals. *Scientific Reports* **7**, 11873.